Tracking Chemical Kinetics in High-Throughput Systems

Hans F. M. Boelens,[a] David Iron,[b] Johan A. Westerhuis,[a] and Gadi Rothenberg*[a]

Abstract: Combinatorial chemistry and high-throughput experimentation (HTE) have revolutionized the pharmaceutical industry—but can chemists truly repeat this success in the fields of catalysis and materials science? We propose to bridge the traditional "discovery" and "optimization" stages in HTE by enabling parallel kinetic analysis of an array of chemical reactions. We present here the theoretical basis to extract concentration profiles from reaction arrays and derive the optimal criteria to follow (pseudo)first-order reactions in time in parallel systems. We use the information vector **f** and introduce in this context the *information gain ratio*, χ_r, to quantify the amount of useful information that can be obtained by measuring the extent of a specified reaction *r* in the array at any given time. Our method is general and independent of the analysis technique, but it is more effective if the analysis is performed online. The feasibility of this new approach is demonstrated in the fast kinetic analysis of the carbon–sulfur coupling between 3-chlorophenylhydrazonopropane dinitrile and β-mercaptoethanol. The theory agrees well with the results obtained from 31 repeated C–S coupling experiments.

Keywords: combinatorial catalysis · high-throughput experimentation · kinetics · reaction arrays · UV/Vis spectroscopy

Introduction

The discovery of new catalysts and the synthesis of new materials have been boosted in the last decade by the introduction of combinatorial and other high-throughput techniques "borrowed" from the pharmaceutical industry.[1] Or have they not? This boost has not yet fulfilled the chemical industry's high expectations, as new catalyst libraries have not yielded dozens of exciting new pathways to produce base chemicals and intermediates.[2] One reason for this is that a host of properties and process conditions must be fine-tuned in order to yield a catalyst that is active, selective, and stable. The new high-throughput experimentation (HTE) techniques are invariably based on a two-step approach comprised of primary screening of a large number of candidates (discovery stage) followed by optimization of a small number of leads. In the discovery stage, thousands or even tens of thousands of catalysts may be tested, but often only one binary parameter is scanned (for example, the product yield may be measured only once for each reaction vessel).[3] Thus, good catalysts may be overlooked and not pass into the optimization stage if they score low, for any reason, in the initial discovery tests, and vice versa.

Figure 1 illustrates the candidate selection process according to the traditional two-stage high-throughput approach. In

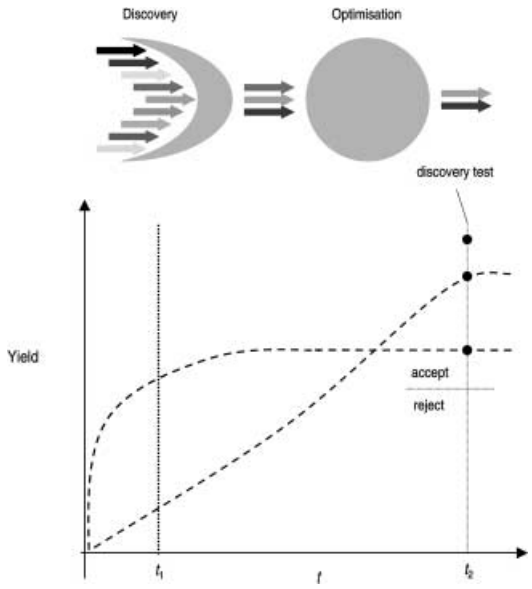

Figure 1. Graphic showing candidate selection according to the traditional two-stage high-throughput approach (top) and the reaction profiles for three candidates (bottom). Good candidates may be mistakenly discarded (and vice versa) if the discovery test is performed at the wrong time.

[a] Dr. G. Rothenberg, H. F. M. Boelens, Dr. J. A. Westerhuis
Chemical Engineering Department, University of Amsterdam
Nieuwe Achtergracht 166, 1018 WV Amsterdam (The Netherlands)
Fax: (+31) 20-525-5604
E-mail: gadi@science.uva.nl

[b] Dr. D. Iron
KdV Institute, University of Amsterdam
Nieuwe Achtergracht 166, 1018 WV Amsterdam (The Netherlands)

Supporting information for this article is available on the WWW under http://www.chemeurj.org or from the author: Annotated MATLAB routine for quick evaluation of high-throughput sampling strategies.

DOI: 10.1002/chem.200304745

this example, a single measurement (the discovery test) is performed for three different catalysts at t_2, giving the results shown by the bold dots. Looking at the reaction profiles (broken lines) we see that it would have been better, in this case, to perform the test at t_1, because then the low initial activity of the red candidate would be observed. Thus, it is crucial to perform the discovery measurement at the correct time, yet this "correct time" is found only when one already knows the kinetic profiles—a time-resolved chicken-and-egg problem.

A possible solution to this problem would be to merge the discovery and the optimization stages by adapting time-resolved analysis to high-throughput environments. Unfortunately, parallel HTE set-ups are ill-suited to quantitative time-resolved analysis: most robotic systems consist of many small and inexpensive reactors and one (expensive) analyzer (Figure 2, below). On-line analysis time becomes the limiting

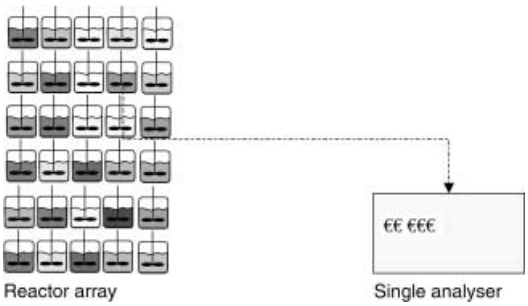

Figure 2. Most common high-throughput experimental set-up used in optimisation studies, in which one expensive analyser is used to monitor an array of reactors sequentially.

factor simply because time does not wait for parallel experimentation. Even in cases when numerous samples can be stored for later off-line analysis, it is essential to determine which samples should be analyzed. To reach these goals and bridge the gap between the discovery and the optimization stages, new concepts in analysis must be realized to complement the HTE robots.[4, 5]

Previously we outlined some approaches to array analysis based on the results of computer simulations.[6] We now present the full theoretical basis required to perform efficient kinetic studies in parallel reaction systems, and demonstrate our approach in the fast analysis of 31 repeats of a carbon–sulfur coupling reaction.

Theory

Concept and assumptions: Let us consider an array of reactors that are all interfaced to one analysis instrument similar to the set-up depicted in Figure 2. Suppose that these reactors are running simultaneously the (pseudo) first-order process A → B, where the initial concentration of A is a_0, the initial concentration of B is 0, the reaction rate constant is k and the concentration of A at time t, a_t, is measured from t_0 to t_∞ (where t_∞ is defined as the time when conversion > 99.5 %). We assume that all of the reactions follow a first-order rate law. Thus, for each reaction in this array, Equation (1) describes the true concentration profile of A

$$a_t = a_0 e^{-kt} \quad (1)$$

Regardless of the analytical technique, the measurement of the extent of a chemical reaction over time always yields a rate constant $\tilde{k}$ which is only an *estimate* of the true rate constant k, and has an error $\Delta\tilde{k}$ which is comprised of systematic (bias) and random parts.[7] Let us assume that the reaction is monitored by spectroscopy. In this case, $\Delta\tilde{k}$ depends both on the experimental set-up and on the way that the spectra are processed. This means that $\Delta\tilde{k}$ is influenced by both the spectroscopic measurement itself[8] and the calibration model used.[9] The concentration estimate $\tilde{a}_t$ obtained at time t has an error $\Delta\tilde{a}_t$. When an adequate calibration model is used, the systematic part of the concentration error will be negligible compared with the random part. Here we will assume that this random concentration error is additive and that it is independently, identically normally distributed (i.i.d.).[10]

If it is not possible to monitor all of the vessels at a given time, a protocol to allocate the analyzer time is needed (we will call this protocol a *sampling strategy*). This can be simple and straightforward (for example, sample each vessel in turn, one after the other) or more complicated (for example, feed back concentration information and sample more frequently those reactions that are changing more rapidly). Figure 3 shows three examples of such sampling strategies.

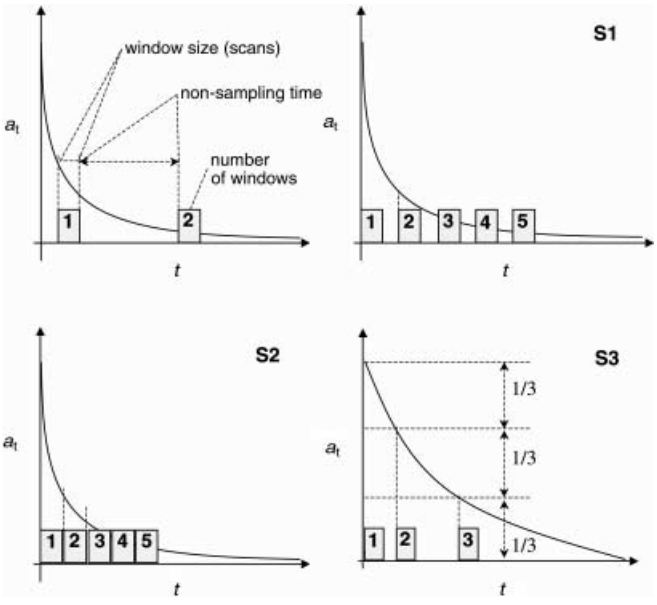

Figure 3. Examples of various sampling strategies with system parameters shown on top left. Strategy S1: equidistant sampling along the time axis. Strategy S2: packing the samples at the start. Strategy S3: even distribution of samples along the concentration axis (example shown with three equidistant samples, the concentration curve is shifted for clarity).

Single- and multiple sampling of first-order reactions: In theory, since a_0 is known, one measurement should suffice to estimate k for each reaction. It is clear a priori that the accuracy of this $\tilde{k}$ would depend on *when* this measurement is

performed. For example, when the measurement is taken immediately after the start of the reaction, $\Delta\tilde{k}$ can be large. This is true even when the error in measuring the concentration is small (cf. the ten concentration profiles shown in Figure 4, that are based on 10 $\tilde{k}$ values with an error in the concentration measurement at $t = 10$ s of only $\pm 0.5\,\%$). We solve this problem by deriving a method to find the optimal time point for a single sample (see Appendix). For a first-order reaction, given that k_0 is an initial guess for k, the best time to measure is at $t = 1/k_0$. This is the same value obtained first by Carr[11] and by Holler et al., in their elegant analysis of random and systematic fluctuations in first-order rate constants.[12] Our purpose, however, is different: We want to lose as little information as possible from the reaction array. The key quantity here is the information value f [Eq. (11), Appendix]. Figure 5, top, shows the change in f^2 as a function of the sampling time. For each measurement time t the height of the curve indicates the accuracy in $\tilde{k}$. The optimal time to measure corresponds to the maximum of the curve ($t = 1/k_0$). The information value f is inversely proportional to the square root of the variance in $\Delta\tilde{k}$ [Eq. (10), Appendix]. This is shown in Figure 5.

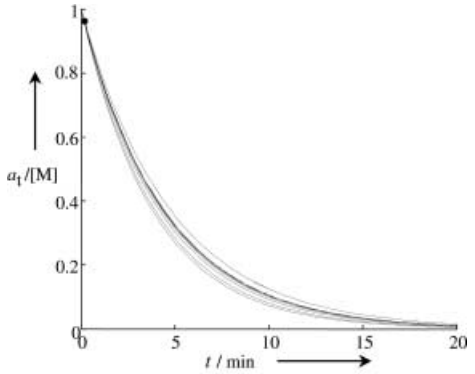

Figure 4. Plot of 10 theoretical first-order reaction profiles, each estimated by taking only one measurement at $t = 10$ s (indicated by a dot). The estimated profiles all start from the same a_0 and the differences are due only to the error of this one measurement. Note that large differences are observed even though the measurement error is only $\pm 0.5\,\%$ of a_0.

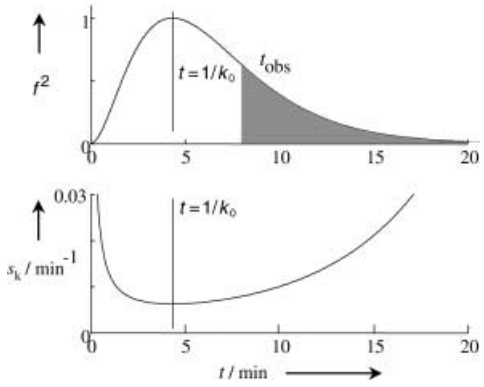

Figure 5. Plot of f^2 for the first-order reaction A → B as a function of time (top) and the change in the standard deviation of $\tilde{k}$ for the same reaction (bottom). The broken lines indicate the optimal sampling time at $t = 1/k_0$. The shaded area on the right is proportional to the improvement in the accuracy of $\tilde{k}$ if one would dedicate all measuring time from t_{obs} onwards to the current reaction.

In practice, however, several measurements are performed for every reaction, and so several sampling strategies are possible (see Figure 3). Deciding which sampling strategy would yield quick yet accurate $\tilde{k}$ values from a large reaction array is far from trivial. For this, we will introduce here a general and fast method to evaluate $\Delta\tilde{k}$. This method also enables easy visual comparison between different sampling strategies.[13]

In high-throughput systems analysis times must be kept short and sample numbers should be confined to a minimum. Again, the curve shown in Figure 5, top, is useful, as the sum of the curve's intensities at the given sampling times is proportional to the "success" of the measurement. For example, if only two samples are taken per reaction, one can see that taking both at the start or at the end of the reaction is not very sensible. The best $\tilde{k}$ values are obtained when both measurements are done at the maximum of the curve, and sampling at time points close to the maximum gives near-optimal results.

A general sampling strategy for high-throughput experimentation: We now extend the above examples to an overall approach for performing kinetic studies in high-throughput systems, where a large number of experiments is performed simultaneously. A good HTE sampling strategy must be able to decide to what reaction the next analyzer time slice should be allocated. Such a strategy should also indicate when the monitoring of a particular reaction is no longer sensible (for example, conversion $> 99\,\%$). For the moment, let us assume that 1) the running reactions are (pseudo) first-order; 2) that some measurements were already performed for each reaction; and 3) that the results of those previously performed measurements are accessible.

At time t_{obs} the system must decide which reaction vessel should be analyzed. Let us number the reaction vessels with an index $r = 1$ to R, and assume that for each reaction N_r measurements are already performed. These N_r measurements yield an estimated rate constant $\tilde{k}_r$. Based on this estimate one can easily quantify the amount of information when the measurement at t_{obs} is actually done for vessel r. This is done by taking the ratio of the f^2 value at t_{obs} to the *sum* of the f^2 values at previous measuring times. We will call this ratio the information gain ratio, χ_r. For each reaction r the value χ_r can be easily calculated using Equation (2), in which $\| \mathbf{f}_{r,\,before} \|^2$ is the sum of the f^2 values at earlier points in time for reaction vessel r [Equation (12), Appendix]. Thus the best investment of analyzer time would be to sample the reaction that has the highest χ_r value.

$$\chi_r = \frac{t_{obs}^2\, e^{-2\tilde{k}_r t_{obs}}}{\| \mathbf{f}_{r,\,before} \|^2} \times 100\,\% \qquad (2)$$

The point in time when it is no longer useful to monitor a given reaction can be determined in several ways. One way is to estimate $\Delta\tilde{k}$ using non-linear regression (or any other method) and check when it drops below a preset limit. Alternatively, one can check whether the remaining area

below the "error" curve (the shaded area in Figure 5) is smaller than a user-defined percentage of the current value of $\tilde{k}$. In other words, to estimate the improvement that one could obtain in the accuracy of k_r if one would dedicate all of the measuring time from now on to reaction r only, and compare this value to a user-defined limit. The advantage of this method, compared with the estimation of $\tilde{k}$ using regression techniques, is that here one can actually look ahead in time rather than backward at what has already been sampled.

Results and Discussion

An experimental example: The carbon–sulfur coupling of 3-chlorophenylhydrazonopropane dinitrile A with β-mercaptoethanol to give the adduct B (Scheme 1) was examined as a model reaction.[14, 15] An excess of β-mercaptoethanol was used to realize pseudo first-order conditions for A → B. The reaction was followed using UV/Vis spectroscopy. 32 Repetitions of this experiment were performed, the first of which was used to estimate the spectra of A and B. 271 UV/Vis spectra were recorded for each experiment, and using these spectra a set of 31 concentration profiles was obtained.

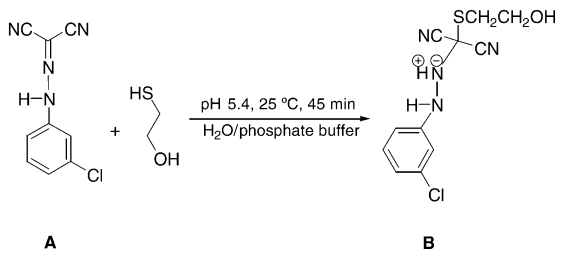

A B

Scheme 1.

We used these repeated experiments to corroborate our theoretical derivations. From the data we estimated 31 $\tilde{k}$ values and calculated their average and standard deviation. As shown below, we found indeed that the standard deviation depends strongly on the sampling time and that lowest standard deviation (i.e., the best estimate of k) is obtained at the optimal sampling time.

The mean of the 31 concentrations of A at $t = 0$ was used as the best estimate of a_0. The kinetic model of Equation (1) was fitted to each measured concentration profile using non-linear regression. The value of a_0 was kept fixed and k was the only parameter. The 31 resulting $\tilde{k}$ values are plotted in Figure 6. These $\tilde{k}$ values are random as no outlying values are found; this confirms that the reactions are well performed. The mean kinetic constant (designated k_{nlin}) equals 0.23 min^{-1}.

We used normalized concentration profiles of A to validate the results derived in the Appendix. The profiles were normalized by dividing each a_t by the initial concentration (a_0). The resulting rth concentration profile is designated $a_r(t_i)$, and for each profile r and each point in time t_i the minimization of the non-linear function in k [Eq. (3)] is performed.

$$\min_k |a_r(t_i) - e^{-kt_i}| \quad (3)$$

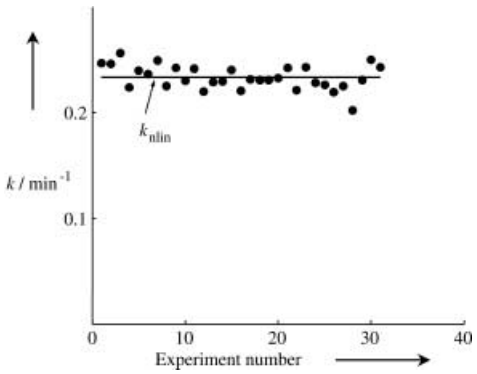

Figure 6. Calculated $\tilde{k}$ values for each of the 31 experiments, determined by non-linear regression. The mean is indicated by the dotted line and designated as k_{nlin}.

This yields a matrix of 31 × 271 $\tilde{k}$ values (note that each of these is based on only one measurement). For each point in time the standard deviation of $\tilde{k}$ is then calculated over the 31 concentration profiles. Figure 7 shows these standard deviations a function of time.

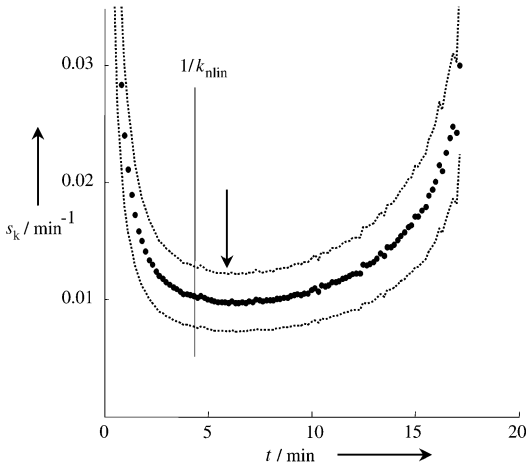

Figure 7. Standard deviation of $\tilde{k}$ (shown as ●) based on the experimental data (each dot is based on 31 $\tilde{k}$ values). The vertical line is drawn at $t = 1/k_{nlin}$ and the arrow indicates the lowest value of s_k. The 95% confidence intervals are shown as dashed lines.

Our theoretical model fits well to the experimental results (cf. Figures 7 and 5). The lowest standard deviation is found at $t = 5$ min 55 s. This is close to $1/k_{nlin}$ (4 min 18 s) considering the flatness of the optimum and the 95% confidence regions. The optimal $\tilde{k}$ is indeed found by sampling at $t \approx 1/k$.

Multiple sampling in high-throughput systems: It would be nice to obtain accurate rate constants which are based on a large number of measurements. However, the size of current reactor arrays and their centralized structure with respect to analysis dictate that no more than, say, four or five measurements should be allowed per reaction. This makes the curve of f^2 a useful visual tool to compare and evaluate different sampling strategies as a function of the number of samples. As an example, let us consider the case for three measurements. The concentration profile for $k = 0.23$ min^{-1} and the points in

time when the measurements are taken are plotted in Figure 8a. The f^2 curve is plotted in Figure 8b, together with the points which correspond to these measurements. Clearly, strategy S3 (see Figure 3) is superior to S1 and S2 (because overall the points are high on f^2 curve) and S2 in this case is the worst (points on the curve are close to zero).

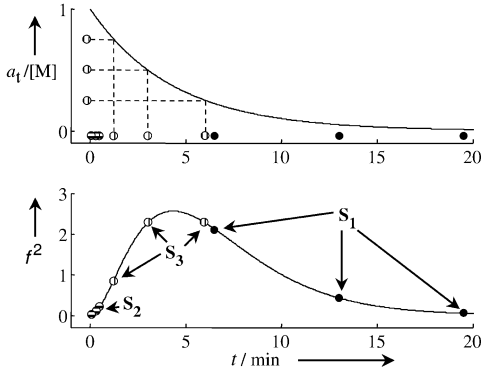

Figure 8. First-order reactant concentration profile (top) and f^2 curve (bottom), used to compare the sampling strategies shown in Figure 3 (example with three measurements).

Examining the performance of the different sampling strategies with respect to the best possible strategy as a function of the number of samples gives even more information. In the ideal case all measurements would be performed at $t = 1/k$. Figure 9 shows that sampling strategy S3 is closest to the best strategy given a *low* number of samples. The performance of S1 (equidistant sampling along the time axis) improves as the number of samples is increases while the performance of S3 deteriorates.

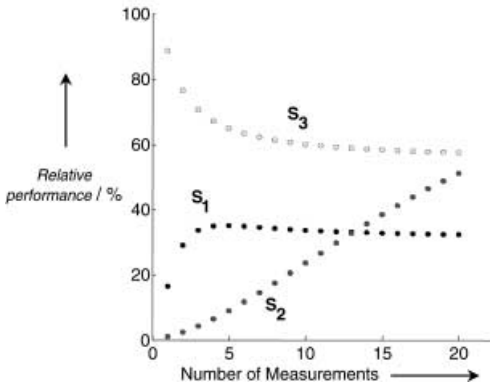

Figure 9. Relative performance of the sampling strategies S_1, S_2, and S_3. The "ideal" sampling strategy (i.e., taking all measurements at $1/k$) is taken as 100%. The sampling window size is 10 s.

Conclusion

New approaches in analysis must be taken in order to realize the goal of high-throughput kinetic studies. In the parallel reactor set-up (the most common to date) it is crucial to find the optimal allocation of the analyzer time. This is even more important in the case of slow analytical methods such as GC and HPLC. To do this, we introduced the information gain ratio, χ_r. Using a reproducible set of experimental data, we show here that χ_r can be applied in various ways. It can be used to quickly assess the performance of different sampling strategies, to decide which reaction in the array can best be monitored at any given time, and to halt the monitoring of a reaction at the right moment.

The examples we show here depict first-order kinetics. The real experimental world, however, is "unfortunately" seldomly first-order. We are extending the above framework to include more complex systems (second-order reactions, cascade reactions, catalyst deactivation, pre-equilibria and Michaelis-Menten kinetics). In the future, the same approach could be used for monitoring biochemical kinetics, determination of NMR relaxation rates,[16] and high-throughput screening of biological functions.

Experimental Section

All chemicals were commercially available (99% pure) and were used without further purification. KH_2PO_4 buffers were purchased from Acros (pro analysis 0.2 M). UV/Vis spectra were recorded using a Hewlett–Packard 8453 spectrophotometer (quartz cuvettes, 1.00 cm path length). Data processing was performed using MATLAB.[17] A detailed description of the sample preparation methods and the experimental apparatus has been published.[14, 15]

A total of 32 identical experiments were performed and monitored using UV/Vis. A stock solution of 3-chlorophenylhydrazonopropane dinitrile A (1.034 M in 0.1 N NaOH) was prepared. For each experiment, part of this stock solution was then diluted to 51.71 μM, buffered to pH 5.4 with KH_2PO_4, and mixed in the quartz cuvette with an excess (276:1 mol:mol) of β-mercaptoethanol solution (2.5 μL β-mercaptoethanol in 7.5 μL KH_2PO_4 buffer solution). UV/Vis spectra of the reaction mixtures were recorded every 10 s at a wavelength range from 300 to 500 nm.

Appendix

Derivation of the optimal design criterion: We start by expanding Equation (1) in a Taylor series around a given initial value k_0 of the kinetic constant [Eq. (4)], wherein R_1 indicates the Lagrangian remainder after a one term Taylor expansion). Then proceed by making the time axis discrete.

$$a^t - a_0 e^{-k_0 t} = -t(k-k_0)\,a_0 e^{-k_0 t} + R_1 \quad (4)$$

The interval along this discrete axis is determined by the time needed by the spectrometer to do one measurement. In general the time axis will therefore be equidistant because the settings of the spectrometer will not be changed during an experiment. However, no such assumption is needed in the derivation below. So, assume that measurements are done at N time points t_1 and define the $(N \times 1)$ vector $\mathbf{t}$ to be $[t_1, t_2, t_3, \ldots t_N]$. Also take the vector $\mathbf{a}$ to contain the measured concentrations at these points in time: $\mathbf{a} = [a(t_1), a(t_2), a(t_3), \ldots a(t_N)]$. Substituting both vectors into Equation (4) gives:

$$\mathbf{a} - a_0 e^{-k_0 t} = -a_0(k-k_0)\,\mathbf{t} \cdot e^{-k_0 t} \quad (5)$$

in which "$\cdot$" is the Hadamard product (element-by-element multiplication) of two vectors. The vector equation can be written in the form:

$$\mathbf{a} - a_0(k_0\mathbf{t} + \mathbf{1}) \cdot e^{-k_0 t} = -a_0 \mathbf{t} \cdot e^{-k_0 t} k \quad (6)$$

or, more simply,

$$\mathbf{y} = \mathbf{f}k \quad (7)$$

where **1** is an $(N \times 1)$ vector of ones, and **y** and **f** are as defined in Equation (8).

$$\mathbf{y} = \mathbf{a} - a_0(k_0\mathbf{t} + \mathbf{1}) \cdot e^{-k_0 t} \quad (8a)$$

$$\mathbf{f} = -a_0 \mathbf{t} \cdot e^{-k_0 t} \quad (8b)$$

Solving Equation (6) is easy when is it viewed as a linear regression problem [see Eq. (7)], in which **y** contains the measured values, **f** contains the errorless ordinate and the scalar k is the parameter to be estimated. The solution[18] to this problem is given by Equation (9), in which T is the transpose operator.

$$k_1 = (\mathbf{f}^T\mathbf{f})^{-1}\mathbf{f}^T\mathbf{y} = \frac{\mathbf{f}^T\mathbf{y}}{\| \mathbf{f} \|^2} \quad (9)$$

Given the initial estimate k_0, Equation (9) supplies the update, k_1, of the reaction rate constant that has the lowest error. Using the assumption about the errors in the measured concentration (see above) and realising that the time values in the vector **t** are error-free, the error structure of **y** is identical to the error structure of **a**. The error in the estimate k_1 is given by Equation (10), in which var(**a**) is variance of the concentration error and var(k_1) is the variance of the estimate of the rate constant.

$$\mathrm{var}(k_1) = \frac{\mathbf{f}^T}{\| \mathbf{f} \|^2}\frac{\mathbf{f}}{\| \mathbf{f} \|^2}\mathrm{var}(\mathbf{a}) = \frac{1}{\| \mathbf{f} \|^2}\mathrm{var}(\mathbf{a}) \quad (10)$$

Note that var(**a**) is a given value that depends on the instrumentation and the calibration model, and that the error in the estimated rate constant is minimized by maximizing the value of $\| \mathbf{f} \|^2$. This result is known in as a D-optimal design.[19] From Equation (8) one can see that the value of $\| \mathbf{f} \|^2$ is determined by the time points (vector **t**) at which the samples are taken.

The best point in time to perform a measurement: Suppose that it is possible to do only one concentration measurement during a reaction. At what point in time should that measurement be performed? In this specific problem the vectors **t** and **f** turn into scalars (t and f) and Equation (8) simplifies to:

$$f = -t a_0 e^{-k_0 t} \quad (11)$$

Maximizing $\| \mathbf{f} \|^2$ is now equivalent to finding the maximum of f^2. A simple calculation shows that there is one maximum, at $t = 1/k_0$.

Evaluation of specific sampling strategies in time: When multiple measurements can be performed on the same reaction, the above approach can be used to evaluate different sampling strategies. Assume, for example, that we wish to compare the two strategies S_x and S_y, start with the same initial estimate k_0. S_x tells us to sample at time points $\mathbf{t}_x$ (an $N_x \times 1$ vector) and S_y consists of doing measurements at points in time $\mathbf{t}_y$ ($N_y \times 1$). We simply compare the values $\| \mathbf{f}_x \|^2$ and $\| \mathbf{f}_y \|^2$. The sampling strategy that yields a higher value is better. When the ratio of the highest value with respect to the lowest is taken, it is even possible to state how much better a specific sampling strategy is. Writing out the expression for $\| \mathbf{f} \|^2$ gives:

$$\| \mathbf{f} \|^2 = \mathbf{f}^T\mathbf{f} = a_0^2 \sum_{i=1}^{N} t_i^2 e^{-2k_0 t_i} \quad (12)$$

The constant a_0 is irrelevant in deciding which strategy is better. The effectiveness of a given sampling strategy may be visualised simply by plotting the sampling times for this sampling strategy on the curve $t^2 e^{-2k_0 t}$.

Acknowledgement

We thank Dr. S. Bijlsma for supplying the UV/Vis measurements.

[1] For an overview see: R. C. Wilson, D. R. Hill, P. R. Gibbs in *High-throughput Synthesis* (Ed.: I. Sucholeiki), Marcel Dekker, New York, **2001**, pp. 271–282; for reviews on HTE applications in materials science see: a) B. Jandeleit, H. W. Turner, T. Uno, J. A. M. Van Beek, W. H. Weinberg, *CATTECH* **1998**, *2*, 101–123; b) T. Bein, *Angew. Chem.* **1999**, *111*, 335–338; *Angew. Chem. Int. Ed.* **1999**, *38*, 323–326; c) F. Schüth, C. Hoffmann, A. Wolf, S. Schunk, W. Stichert, A. Brenner, *Comb. Chem.* **1999**, 463–477; d) H. B. Kagan, *J. Organomet. Chem.* **1998**, *567*, 3–6; in heterogeneous catalysis e) S. Senkan, *Angew. Chem.* **2001**, *113*, 322–341; *Angew. Chem. Int. Ed.* **2001**, *40*, 312–329; f) A. Holzwarth, P. Denton, H. Zanthoff, C. Mirodatos, *Catal. Today* **2001**, *67*, 309–318; in biocatalysis g) M. T. Reetz, *Angew. Chem.* **2001**, *113*, 292–320; *Angew. Chem. Int. Ed.* **2001**, *40*, 284–310.

[2] a) R. Schlögl, *Angew. Chem.* **1998**, *110*, 2467–2470; *Angew. Chem. Int. Ed.* **1998**, *37*, 2333–2336; b) R. Hoffmann, *Angew. Chem.* **2001**, *113*, 3439–3443; *Angew. Chem. Int. Ed.* **2001**, *40*, 3337–3340.

[3] a) P. Claus, D. Honicke, T. Zech, *Catal. Today* **2001**, *67*, 319–339; b) C. de Bellefon, N. Tanchoux, S. Caravieilhes, P. Grenouillet, V. Hessel, *Angew. Chem.* **2001**, *112*, 3584–3587; *Angew. Chem. Int. Ed.* **2000**, *39*, 3442–3445; c) C. de Bellefon, N. Tanchoux, S. Caravieilhes, *J. Organomet. Chem.* **1998**, *567*, 143–150; d) M. T. Reetz, K. M. Kuhling, S. Wilensek, H. Husmann, U. W. Hausig, M. Hermes, *Catal. Today* **2001**, *67*, 389–396.

[4] For a discussion on the experimental design of HTE see M. W. Lutz, J. A. Menius, T. D. Choi, R. G. Laskody, P. L. Domanico, A. S. Goetz, D. L. Saussy, *Drug Discovery Today* **1996**, *1*, 277–286.

[5] a) F. W. J. van den Berg, H. F. M. Boelens, H. C. J. Hoefsloot, A. K. Smilde, *AIChE J.* **2001**, *47*, 2503–2514; b) A. K. Smilde, H. C. J. Hoefsloot, F. W. J. van den Berg, *Anal. Chem.* **2002**, *74*, 3105–3111.

[6] G. Rothenberg, H. F. M. Boelens, D. Iron, J. A. Westerhuis, *Catal. Today* **2003**, *81*, 359–367.

[7] For an overview see D. L. Massart, B. G. M. Vandeginste, L. M. C. Buydens, S. de Jong, J. Smeyers-Verbeke, *Handbook of Chemometrics and Qualimetrics*, Elsevier, Amsterdam, **1997**, pp. 393–396.

[8] Spectra can be measured either with dispersive or with Fourier transform spectrometers. In both cases the spectrum is based on a "window" comprised of a number of scans averaged over time. This time averaging increases the signal-to-noise (S/N) ratio. However, the disadvantage of increasing the number of scans per window is that the total time needed to collect one spectrum also increases and meanwhile the reaction continues and concentrations change.

[9] A calibration model must be applied to the measured spectrum to estimate concentrations. The error of these estimates depends on the model because any calibration model is based on spectroscopic and reference measurements pertaining to a finite number of calibration samples. See a) H. Martens, T. Naes, *Multivariate Calibration*, Wiley, New York, **1989**; b) P. Geladi, *Chemom. Intell. Lab. Sys.* **2002**, *60*, 211–224.

[10] The random error, $\Delta\tilde{a}_t$, at each point in time is assumed to be $N(0,\sigma)$ distributed. Furthermore, errors at subsequent points in the time are assumed to be statistically independent. And finally, the measured concentration $\tilde{a}_t$ is taken to be equal to $a_t + \Delta\tilde{a}_t$. So, the concentration error is additive and independent of the concentration level.

[11] P. W. Carr, *Anal. Chem.* **1978**, *50*, 1602–1607.

[12] a) F. J. Holler, R. K. Calhoun, S. F. McClanahan, *Anal. Chem.* **1982**, *54*, 755–761.

[13] When multiple samples are taken the information vector **f** replaces f. The sampling strategy that yields the highest value for $\| \mathbf{f} \|^2$ gives the best $\tilde{k}$ (see Appendix).

[14] S. Bijlsma, D. J. Louwerse, A. K. Smilde, *J. Chemometrics* **1999**, *13*, 311–329.

[15] S. Bijlsma, H. F. M. Boelens, H. C. J. Hoefsloot, A. K. Smilde, *Anal. Chim. Acta* **2000**, *419*, 197–207.

[16] J. A. Jones, P. Hodgkinson, A. L. Barker, P. J. Hore, *J. Magn. Reson. B* **1996**, *113*, 25–34.

[17] MATLAB is commercially available from MathWorks, Natick USA, Version 6.1, **2001**.

[18] N. R. Draper, H. Smith, *Applied Regression Analysis*, Wiley, New York, **1998**.

[19] A. C. Atkinson, A. N. Donev, *Optimal Experimental Designs*, Clarendon Press, Oxford, **1992**.

Received: January 20, 2003 [F4745]

